Electronic Supplementary Material (ESI) for Polymer Chemistry.

Supporting Information to

BiTEMPS Methacrylate Dynamic Covalent Cross-linker Providing Rapid Reprocessability and Extrudability of Covalent Adaptable Networks: High-Yield Synthesis with Strong Selectivity for Disulfide Linkages

Tapas Debsharma,[a,+] Nathan S. Purwanto,[b,+] Logan M. Fenimore,[a] Sarah Mitchell,[c]

Jayme Kennedy,[c] and John M. Torkelson[a,b,*]

[a]Department of Chemical and Biological Engineering,

[b]Department of Materials Science and Engineering,

Northwestern University, Evanston, IL 60208, USA.

[c]Braskem America, 550 Technology Drive, Pittsburgh, PA 15219, USA

[+]co-first authors

[*]Corresponding author, e-mail: j-torkelson@northwestern.edu

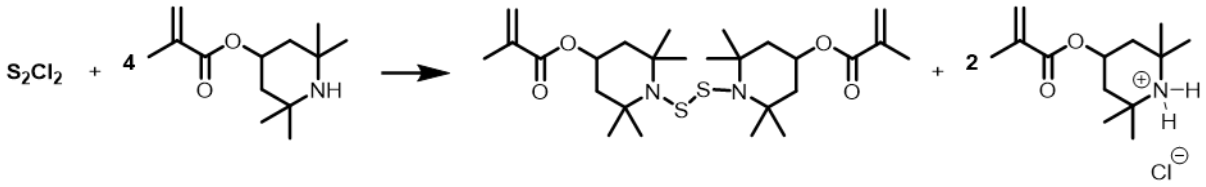

Scheme S1. Balanced equation for the synthesis of BTMA-S2.

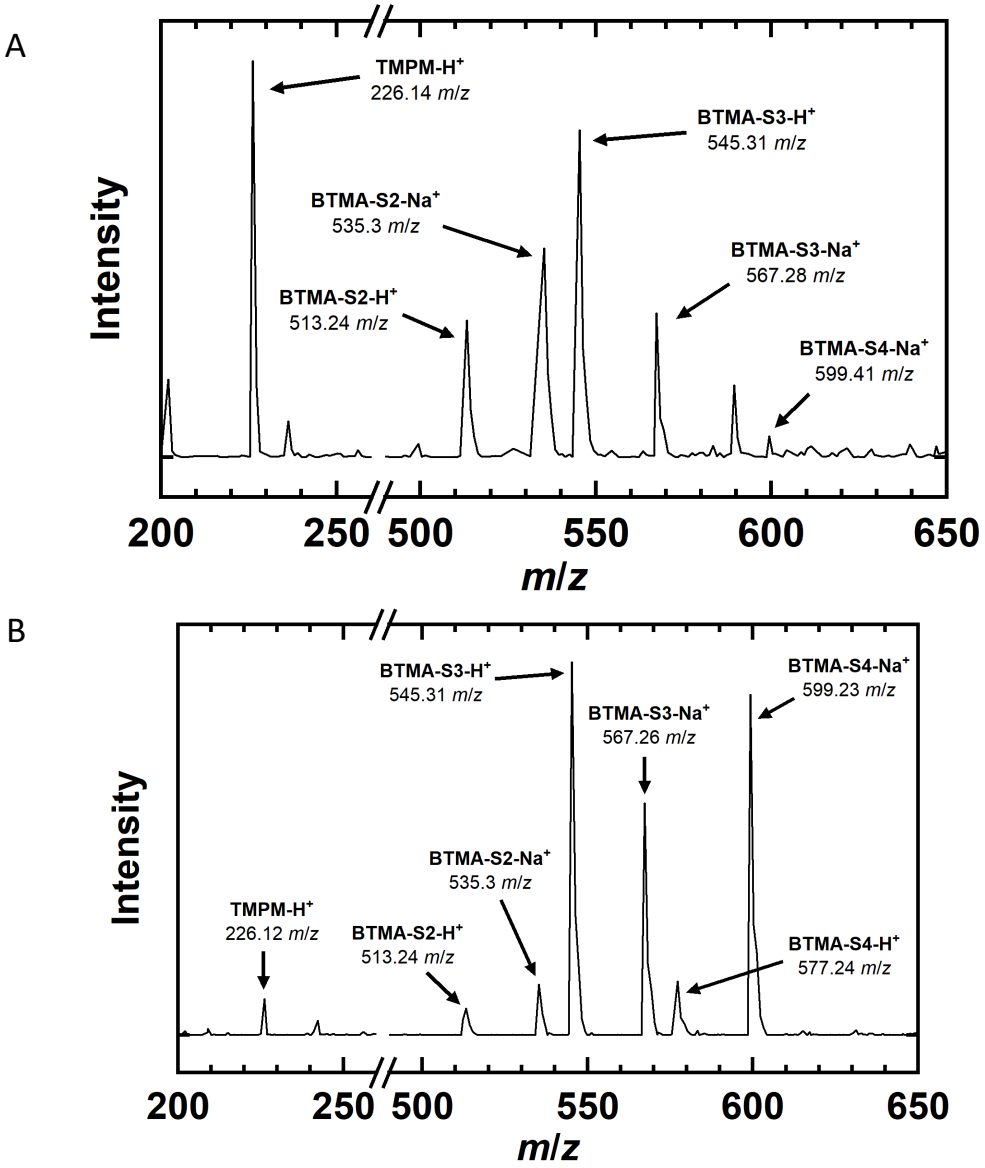

Figure S1. (A/B) ESI-MS spectra of BTMA-S_n products from two different syntheses. In addition to the presence of disulfide (BTMA-S2), both spectra show the presence of protonated TMPM (TMPM-H^+). One spectrum (B) clearly shows the presence of BTMA-S3 and BTMA-S4 while the other (A) clearly shows the presence of BTMA-S3, with a BTMA-S4 peak at slightly above noise level.

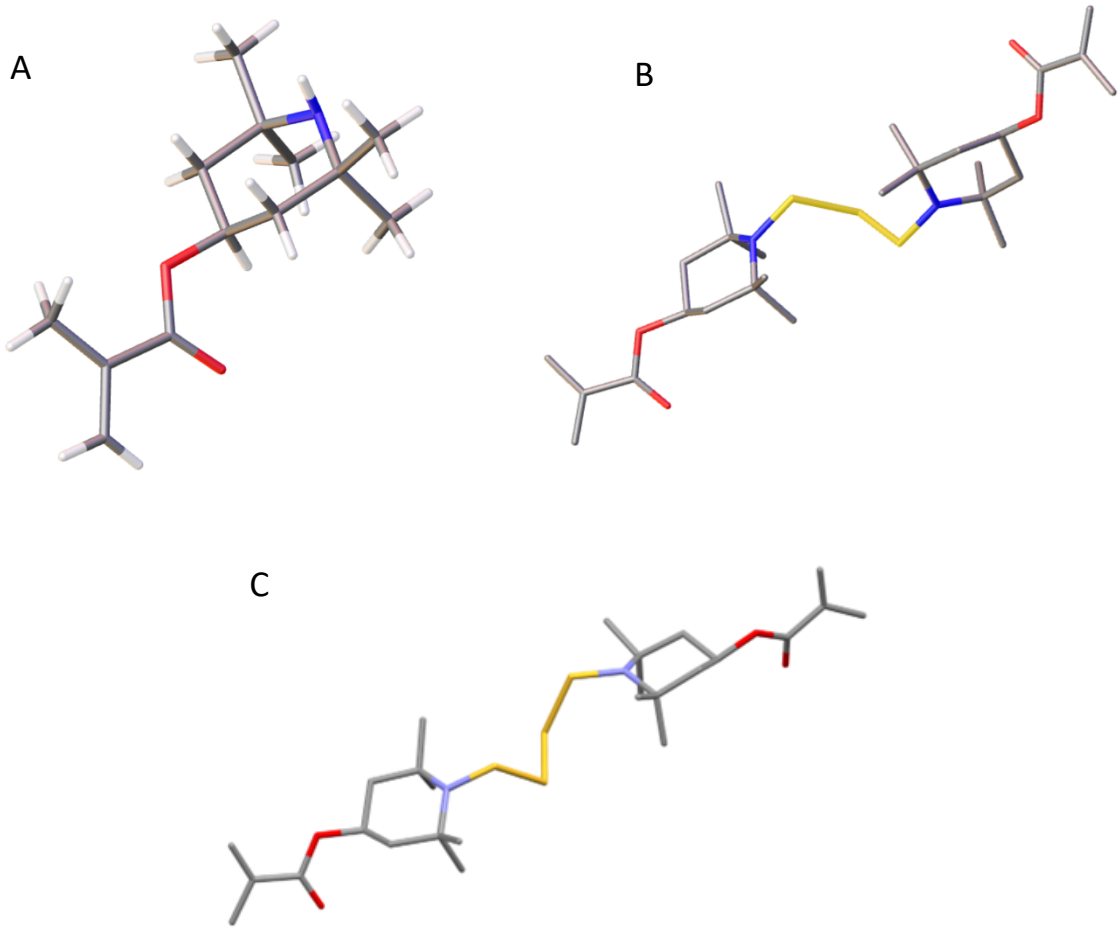

Figure S2. Unit cells of three crystals from BTMA-S_n samples measured in single-crystal X-ray crystallography: (A) unreacted TMPM, (B) BTMA-S3, (C) BTMA-S4. Grey, white, red, purple, and yellow represent carbon, hydrogen, oxygen, nitrogen, and sulfur atoms, respectively. Hydrogens were removed from BTMA-S3 and BTMA-S4 for clarity.

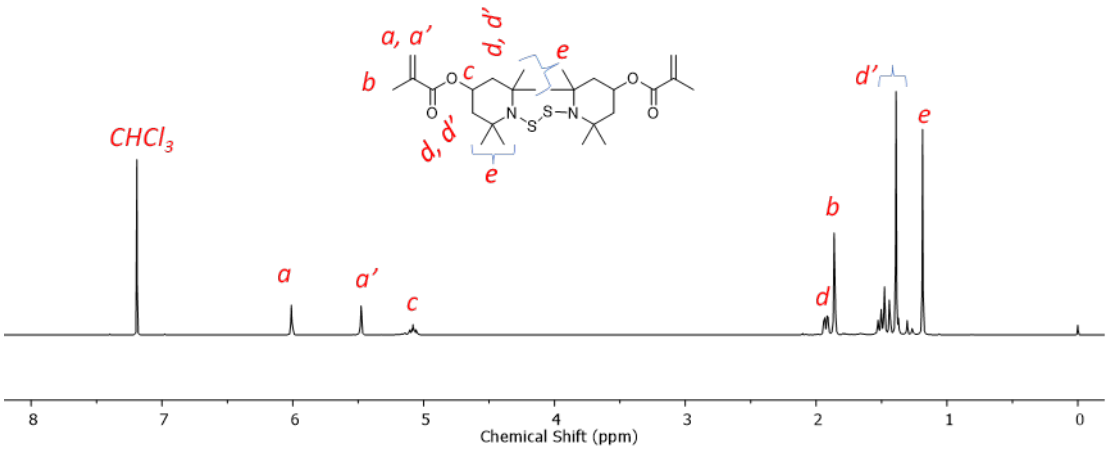

Figure S3. ^{1}H NMR ($CDCl_3$, 500 MHz) of crude BTMA-S2 synthesized in dry DCM at -70 °C.

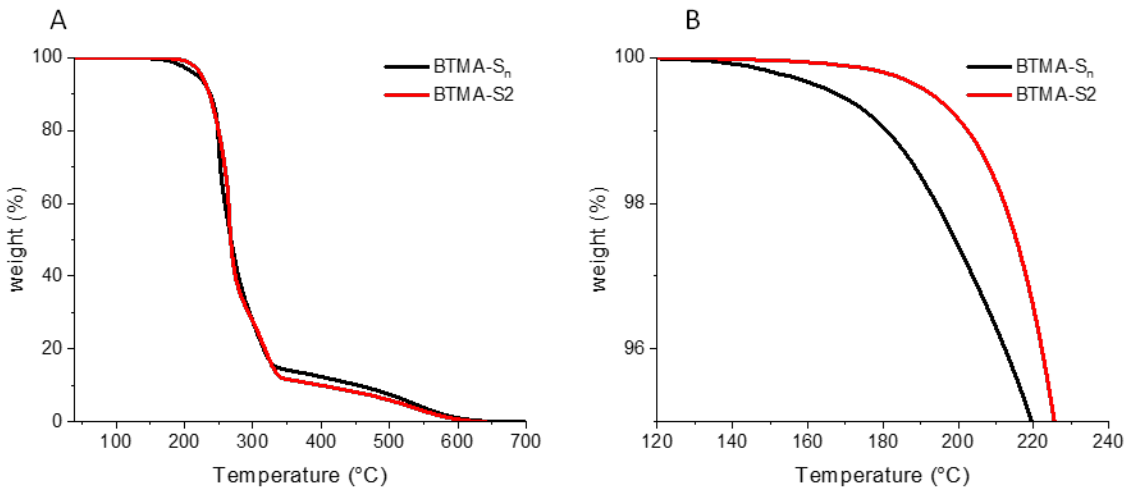

Figure S4. TGA thermogram of BTMA-S_n and BTMA-S2: A) normalized weight as a function of temperature from 40 °C to 700 °C. B) Normalized weight from 100 % to 95 % as a function of temperature from 120 °C to 240 °C.

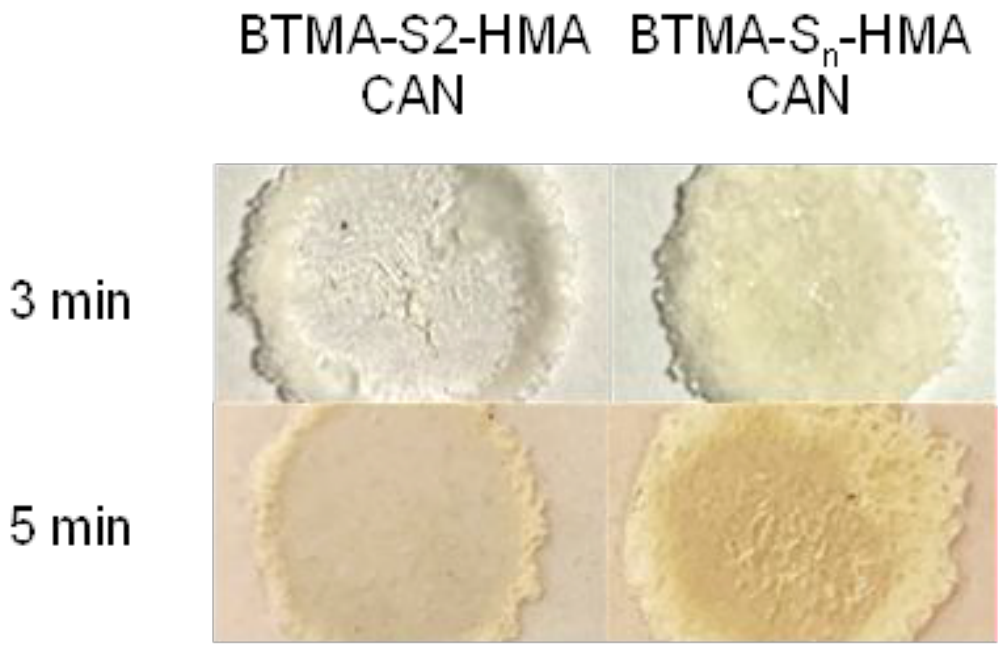

Figure S5. Images of compression-molded samples of BTMA-S2-HMA CAN and BTMA-S_n-HMA CAN at 130 °C and 10 MPa after 3 min and 5 min.

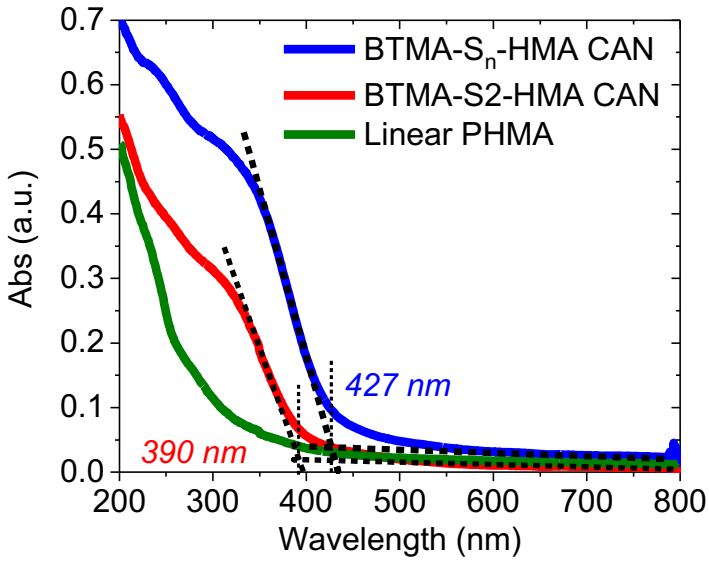

Figure S6. UV-Vis diffuse reflectance spectroscopy of BTMA-S2-HMA CAN and BTMA-S$_n$-HMA CAN materials.

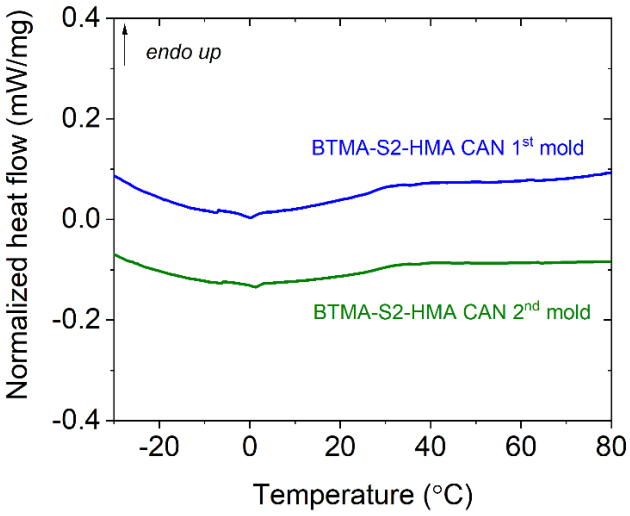

Figure S7. DSC thermograms of 1st and 2nd compression molded BTMA-S2-HMA CAN.

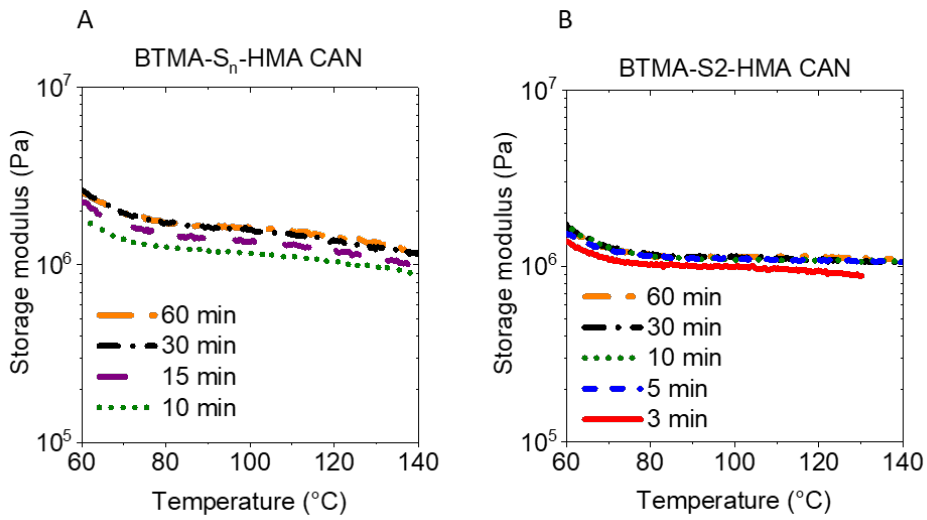

Figure S8. Storage modulus (in log scale) as a function of temperature of samples compression molded at different times: A) BTMA-S$_n$-HMA CAN and B) BTMA-S2-HMA CAN.

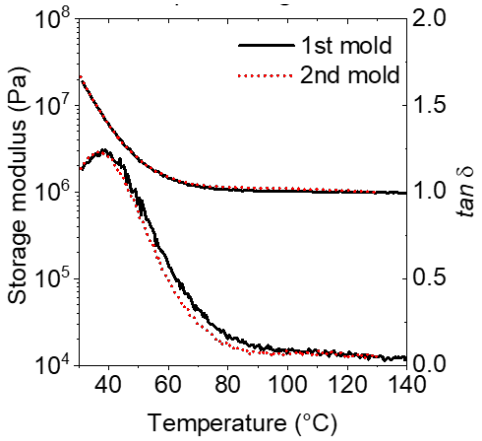

Figure S9. Storage modulus as a function of temperature for the 1st and 2nd reprocessed BTMA-S2-HMA CAN samples obtained after compression molding at 130 °C for 5 min.

Figure S10. Image of twin-screw extruder instrument used in this study (Thermo Scientific Haake MiniLab 3)

Table S1. Storage modulus (*E'*) as a function of temperature for reprocessed BTMA-S2-HMA CAN and BTMA-S_n-HMA CAN samples obtained from compression molding at 130 °C for 60 min.

E' (MPa)	90 °C	100 °C	110 °C	120 °C	130 °C	140 °C
BTMA-S_n-HMA CAN (1^{st} mold)	1.66 ± 0.12	1.62 ± 0.04	1.56 ± 0.06	1.48 ± 0.03	1.33 ± 0.07	1.23 ± 0.10
BTMA-S_n-HMA CAN (2^{nd} mold)	1.68 ± 0.12	1.66 ± 0.07	1.57 ± 0.03	1.52 ± 0.12	1.38 ± 0.09	1.28 ± 0.09
BTMA-S2-HMA CAN (1^{st} mold)	1.11 ± 0.05	1.11 ± 0.04	1.12 ± 0.08	1.12 ± 0.09	1.10 ± 0.06	1.08 ± 0.10
BTMA-S2-HMA CAN (2^{nd} mold)	1.09 ± 0.06	1.10 ± 0.11	1.10 ± 0.14	1.11 ± 0.09	1.10 ± 0.03	1.07 ± 0.10
BTMA-S2-HMA CAN (extrudate)	1.11 ± 0.05	1.11 ± 0.04	1.14 ± 0.08	1.18 ± 0.09	1.20 ± 0.06	1.25 ± 0.10

Table S2. Characteristic relaxation times (τ^*), stretching exponent (β), average relaxation times ($\langle\tau\rangle$), and Arrhenius activation energy (E_a) values from stress relaxation measurements of 1^{st} compression molded samples of BTMA-S2-HMA CAN and BTMA-S_n-HMA CAN materials at different temperatures.

Sample	T (°C)	τ^* (s)	β	$\langle\tau\rangle$ (s)	R^2	E_a (kJ/mol)	R^2
BTMA-S2-HMA CAN	130	128	0.79	146	0.999	102 ± 4	0.999
	140	57	0.79	65	0.989		
	150	29	0.82	32	0.997		
	160	15	0.81	16	0.998		
BTMA-S_n-HMA CAN	120	1090	0.72	1350	0.999	107 ± 3	0.997
	130	422	0.73	514	0.998		
	140	168	0.79	192	0.997		
	150	62	0.91	67	0.997		